European Journal of Pharmaceutics and Biopharmaceutics 85 (2013) 898–910

Contents lists available at SciVerse ScienceDirect

European Journal of Pharmaceutics and Biopharmaceutics

journal homepage: www.elsevier.com/locate/ejpb

Research paper

Unique SERM-like properties of the novel fluorescent tamoxifen derivative FLTX1 ☆

Jorge Marrero-Alonso [a,b], Araceli Morales [c], Benito García Marrero [d], Alicia Boto [b,d], Raquel Marín [b,c], Débora Cury [c], Tomás Gómez [a,b], Leandro Fernández-Pérez [b,e], Fernando Lahoz [f], Mario Díaz [a,b,*]

[a] Departamento de Biología Animal, Universidad de La Laguna, Tenerife, Spain
[b] Instituto Canario de Investigación del Cáncer (ICIC), Spain
[c] Departamento de Fisiología, Universidad de La Laguna, Tenerife, Spain
[d] Instituto de Productos Naturales y Agrobiología, CSIC, Tenerife, Spain
[e] Departamento de Ciencias Clínicas, Universidad de Las Palmas de Gran Canaria, Spain
[f] Departamento Física Fundamental y Experimental, Electrónica y Sistemas, Universidad de La Laguna, Tenerife, Spain

ARTICLE INFO

Article history:
Received 14 December 2012
Accepted in revised form 30 April 2013
Available online 31 May 2013

Keywords:
Selective estrogen receptor modulators (SERMs)
Estrogen receptor-positive breast cancer
Antiestrogens
Fluorescent derivatives
Estrogen-dependent cell proliferation
Reporter-based transcriptional activity
Uterotrophic effects

ABSTRACT

Tamoxifen is a selective estrogen receptor modulator extensively used on estrogen receptor-positive breast cancer treatment. However, clinical evidences demonstrate the increased incidence of undesirable side effects during chronic therapies, the most life threatening being uterine cancers. Some of these effects are related to tissue-dependent estrogenic actions of tamoxifen, but the exact mechanisms remain poorly understood. We have designed and synthesized a novel fluorescent tamoxifen derivative, FLTX1, and characterized its biological and pharmacological activities. Using confocal microscopy, we demonstrate that FLTX1 colocalizes with estrogen receptor α (ERα). Competition studies showed that FLTX1 binding was totally displaced by unlabeled tamoxifen and partially by estradiol, indicating the existence of non-ER-related triphenylethylene-binding sites. Ligand binding assays showed that FLTX1 exhibits similar affinity for ER than tamoxifen. FLTX1 exhibited antiestrogenic activity comparable to tamoxifen in MCF7 and T47D cells transfected with 3xERE-luciferase reporter. Interestingly, FLTX1 lacked the strong agonistic effect of tamoxifen on ERα-dependent transcriptional activity. Additionally, *in vivo* assays in mice revealed that unlike tamoxifen, FLTX1 was devoid of estrogenic uterotrophic effects, lacked of hyperplasic and hypertrophic effects, and failed to alter basal *proliferating cell nuclear antigen* immunoreactivity. In the rat uterine model of estrogenicity/antiestrogenicity, FLTX1 displayed antagonistic activity comparable to tamoxifen at lower doses, and only estrogenic uterotrophy at the highest dose. We conclude that the fluorescent derivative FLTX1 is not only a suitable probe for studies on the molecular pharmacology of tamoxifen, but also a potential therapeutic substitute to tamoxifen, endowed with potent antiestrogenic properties but devoid of uterine estrogenicity.

© 2013 Elsevier B.V. All rights reserved.

1. Introduction

Tamoxifen is a nonsteroidal agent that competitively binds to estrogen receptors (ER) and competes with estrogen, the cognate ligand, for the ER binding sites. The antiestrogenic properties of tamoxifen in breast and other tissues are associated with its ability to halt transcriptional activation of estrogen-responsive genes that govern cellular proliferation [1]. Tamoxifen itself is a prodrug, having relatively little affinity for ER. However, when metabolized in the liver by the cytochrome P450 (CYP2D6 and CYP3A4), tamoxifen is transformed into the active metabolites 4-hydroxytamoxifen and N-desmethyl-4-hydroxytamoxifen (endoxifen), which have 30–100 times more affinity with the estrogen receptor than tamoxifen itself [2].

Hormone therapies for the treatment of estrogen receptor-positive breast cancers have evolved since their origin in the 1970s. However, in spite of the constant search for novel antiestrogenic drugs and selective estrogen receptor modulators (SERMs) [1,3–7], tamoxifen has been for a long time almost the only low cost hormonal option for the systemic treatment of pre-menopausal patients [8,9]. Nevertheless, due to the increase in endometrial cancer and thromboembolic events in tamoxifen therapies [9–11], serious concerns exist on its use for cancer prevention or long-term palliative treatment. Furthermore, numerous studies have shown

☆ *Disclosures:* FLTX1 has been registered as patent # ES2498.5 at the Spanish Office of Patents and Marks.

* Corresponding author. Laboratorio de Fisiología y Biofísica de Membranas, Departamento de Biología Animal, Facultad de Biología, Universidad de La Laguna, 38206 Tenerife, Spain. Tel.: +34 922 318343; fax: +34 922 318411.
E-mail address: madiaz@ull.es (M. Díaz).

0939-6411/$ - see front matter © 2013 Elsevier B.V. All rights reserved.
http://dx.doi.org/10.1016/j.ejpb.2013.04.024

that tamoxifen is able to exert non-genomic effects acting through different molecular targets that result in both beneficial and undesirable side effects [reviewed in 12,13]. These actions occur through mechanisms still poorly understood, partly due to the lack of appropriate experimental tools to identify specific tamoxifen targets.

In the last decade, alternative treatments for estrogen-dependent breast cancer have been focused on the development of aromatase inhibitors, which arrest the production of estrone, the principal estrogen in post-menopausal women. The clinical trials have shown that aromatase inhibitors are effective in reducing the mortality associated with ER-positive breast cancer although the overall survival is not superior to that provided by tamoxifen [14,15]. The available evidence for receptor-positive breast cancer in post-menopausal women strongly supports the combined use of tamoxifen and aromatase inhibitors.

In line with this philosophy, in the last decade, we have designed and synthesized a set of novel tamoxifen derivatives, some of them as fluorescent probes. Based on the accumulated knowledge on the structure–activity of different triphenylethylene derivatives studied so far [12,16], and the molecular determinants of antiestrogenic action of tamoxifen [17,18], we have modified the dimethylaminoethoxy side chain of tamoxifen by partial demethylation and attachment to a NBD (7-nitrobenzo[c][1,2,5]oxadiazol-4-yl) fluorescent tag. Moreover, the basic amine of demethyltamoxifen (NDTx) allowed us the attachment of the NBD group without a linker chain, while the triphenyl core of tamoxifen remained unaltered, which is an absolute requirement for its binding to estrogen receptors [16–18].

We show that this novel fluorescent triphenylethylene derivative, FLTX1, specifically labels intracellular tamoxifen-binding sites, including ERα, and displays unique pharmacological properties both *in vitro* and *in vivo*. Thus, while FLTX1 exhibits the potent antiestrogenic properties of tamoxifen in breast cancer cells, it is devoid of the estrogenic agonistic effect on the uterus, a feature responsible for the most worrisome side effect of tamoxifen: womb cancers.

2. Materials and methods

Detailed Section 2 is available in Supplementary material. Animal procedures and the overall study complied with Spanish and EU animal care guidelines (RD 1201/2005, directive 2003/65/CE) and were approved by the ethics committee of University of La Laguna.

2.1. Synthesis of N-(7-nitrobenzo[c][1,2,5]oxadiazol-4-yl)demethyltamoxifen (FLTX1)

FLTX1 was synthesized from commercial tamoxifen (Tx, purity ⩾99%, Sigma–Aldrich) in two sequential steps (Fig. 1A). Initially, tamoxifen was demethylated to produce *N*-demethyltamoxifen, and then, 4-chloro-7-nitro-1,2,3-benzoxadiazole (NBD-Cl) was covalently bound to the secondary amine in *N*-demethyltamoxifen to form *N*-(7-nitrobenzo[c][1,2,5]oxadiazol-4-yl)demethyltamoxifen (FLTX1). The detailed procedure for the synthesis is described in Supplementary information S1. Normalized FLTX1 spectra showed maximal excitation and emission peaks centered at 476 nm and 527 nm, respectively (Fig. 1C).

2.2. Fluorescent labeling of cell cultures

Detailed cell culture procedures for the different cell lines used in this study are explained in Supplementary information S2. ER-positive MCF7 cells were fixed under non-permeabilizing conditions in 2% paraformaldehyde/0.1% glutaraldehyde/150 mM sucrose for 30 min at RT. To permeabilize the plasma membrane, cells were fixed in the presence of 0.5% NP-40 for 2 min. Cells were then incubated for 2 h at RT in the presence of 50 μM FLTX1. In competition assays, prior to the addition of FLTX1, cultures were exposed to different concentrations of Tx or 17β-estradiol (E2, Sigma–Aldrich) for 30 min at RT. For colocalization analysis of FLTX1 with ERα, fixed cells were first incubated with MC-20 polyclonal anti-ERα (Santa Cruz Biotechnology), followed by incubation with a corresponding Alexa 514-coupled secondary antibody (Invitrogen). Then, cells were incubated with 50 μM FLTX1 and mounted for visualization. For nuclear staining, cells were exposed to 300 nM DAPI (Invitrogen) in PBS for 5 at RT.

Results were visualized by confocal microscopy (Olympus FV1000), selecting the 458 nm line for FLTX1 excitation and the 515 nm line for Alexa Fluor 514-coupled antibody. Olympus FluoView software 2.1 was used for image processing. Quantitative values of competitive assays were referred to the percentage of pixel intensity in cells exposed to FLTX1 alone.

2.3. Estrogen receptor competitive binding assay

Estrogen receptor was obtained from uterine cytosol fraction from mature female Sprague–Dawley rats (Supplementary material S2). Aliquots of 100 μl cytosol were incubated with 5 nM [^{3}H]E_2 and increasing concentrations of unlabeled competitors (0.1 nM–100 μM) for 18 h at 4 °C. Then, 200 μl of dextran-coated charcoal suspension (0.8% charcoal: 0.08% dextran) in TRIS–EDTA–Glycerol–Mg buffer was added to each tube and incubated for 10 min. The charcoal was then centrifuged at 3000*g* for 10 min. Supernatant was measured for radioactivity in 4 ml scintillation cocktail Optiphase Hisafe 2 (PerkinElmer) by LKB WALLAC 1214-Rackbeta counter (LKB Instrument). Corrections were made for non-specific binding. Relative binding affinity (RBA) of FLTX1 was calculated as the ratio of FLTX1 and Tx IC_{50} values as derived from dose–response curves.

2.4. Cell proliferation assays

MCF7 cells were seeded at 1×10^4 cells per well in 0.1 ml of phenol red-free DMEM (BioWhittaker) with 10% dextran-charcoal treated FBS (Linus, Cultek). 24 h after seeding, Tx and FLTX1 were applied alone for the estrogenic/toxicity 6 days assessments. In antiestrogenic assays, 100 pM E2 was added 24 h after preincubation with Tx or FLTX1 and incubated for additional 4 days (see details in Supplementary material S2). Cell viability was measured using the Cell Proliferation Reagent WST-1 (Roche).

2.5. Transcriptional activity studies

Transcriptional activity was measured by a luciferase-based reporter gene assay in three breast cancer cell lines expressing different nuclear receptors: MCF7 cells transiently transfected with 3x-Vit-ERE-TATA-luciferase reporter, T47D-KBluc cells stably transfected with the pGL2.TATA.Inr.luc.neo [19], and MDA-kb2 cells that stably express the pMMTV.neo.luc reporter gene construct, androgen receptor, and glucocorticoid receptor [20].

Cells were plated in 12 well plates. The following day, selected doses of Tx or FLTX1 were added to 1 ml of fresh media for antagonistic pre-treatment. After 8 h of incubation, media was replaced with the corresponding treatments: for antagonistic assessment, transiently transfected MCF7 cells and T47D-KBluc cell line were incubated with Tx or FLTX1 plus 100 pM E2. For agonistic assessment, cells were incubated only with Tx or FLTX1. Cells were incubated overnight (15–16 h) with treatments before processing for luciferase activity. Further details about transfection procedures

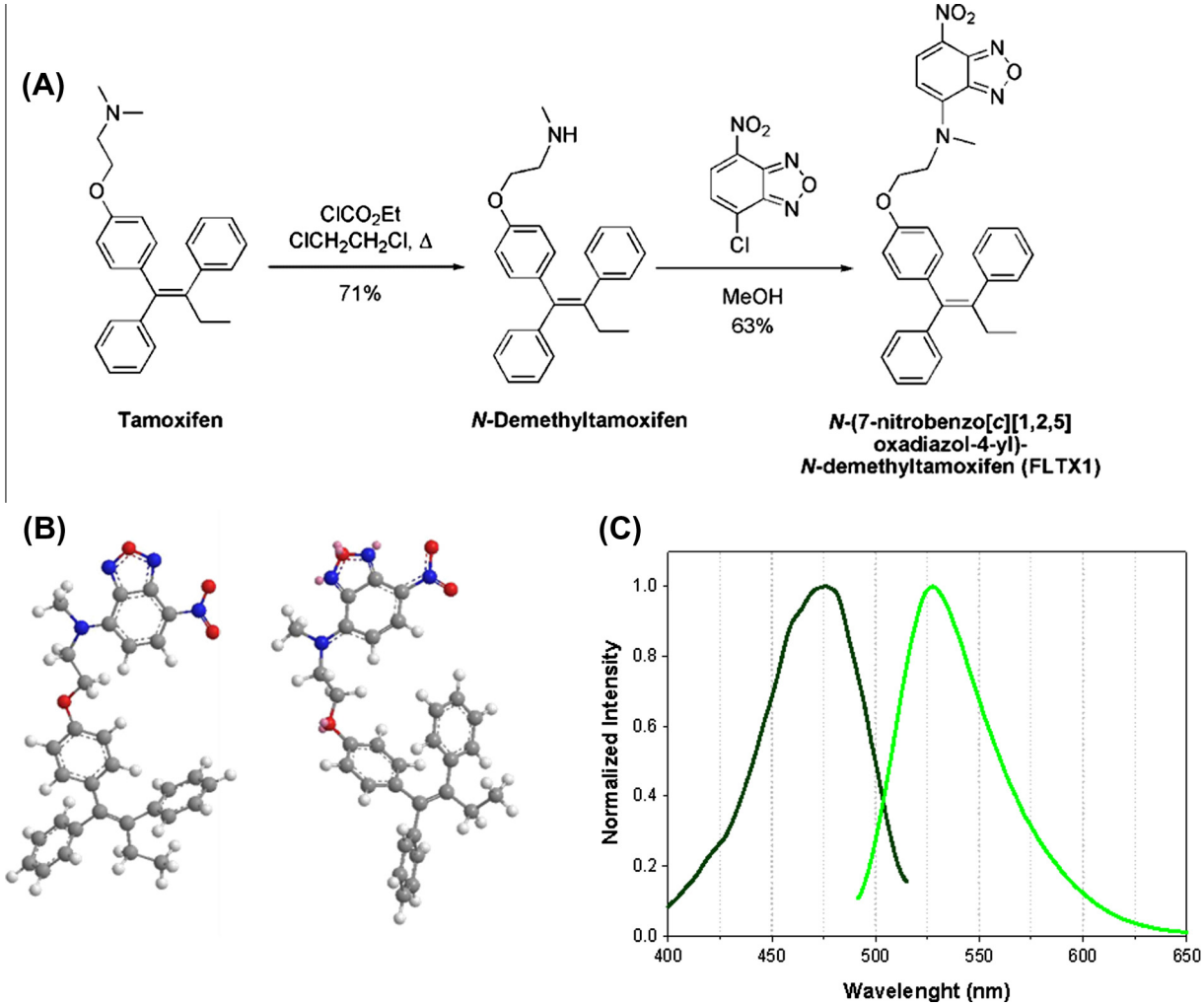

Fig. 1. (A) Synthesis of *N*-(7-nitrobenzo[c][1,2,5]oxadiazol-4-yl)demethyltamoxifen (FLTX1) from Tx. (B) Ball-and-stick representations of FLTX1 minimum-energy conformations. (C) Fluorescent spectral features of FLTX1 (1 mM) dissolved in methanol. (For interpretation of the references to color in this figure legend, the reader is referred to the web version of this article.)

for transcriptional assays are explained in Supplementary material S2.

2.6. In vivo uterotrophic bioassays

Immature female CD-1 mice and Sprague–Dawley rats were subcutaneously injected with, respectively, 10 or 5 ml/kg of an olive oil solution of Tx or FLTX1, with or without 0.5 μg/kg ethinyl estradiol (EE, Sigma–Aldrich) only in case of rats. For CD-1 mice, Tx and FLTX1 were used at doses of 0.01, 0.1, and 1 mg/kg/day, and for Sprague–Dawley rats, an additional dose of 10 mg/kg/day was included. Animals were injected for 3 consecutive days. A subset of animals was subcutaneously treated during the same 3 days period with vehicle (negative control), or 1 μg/kg E2 (mice) or 0.5 μg/kg EE (rats) as a positive internal controls. A minimum of four animals per dose were used.

Approximately 24 h after the last injection, animals were sacrificed and dissected. Wet and blotted uterus, uterine horns, luminal fluid, vaginal, cervical, liver, and spleen weights were obtained. Tissue weight/body weight ratios were calculated for each animal. For each uterus, one horn was fixed in Bouin's fixative and the other in 4% paraformaldehyde in phosphate buffered saline (pH 7.4) and processed for histological and morphometrical examination.

2.7. Histological and morphometrical studies

Following fixation, the uterine tissues of mice were embedded in paraffin, cut longitudinally or crosswise with a microtome in 10 μm-thick sections, and mounted onto slides. Sections exposed to Bouin's fixative were deparaffinized, stained with hematoxylin and eosin, and processed for morphometrical analyses. Histological markers of uterotrophy included epithelial cell height, and epithelial cell number in longitudinally sections, and gland number in cross sections of uterine mid-region. These parameters were quantified in, at least, three areas of 300 μm^2 of three different sections for each animal.

Sections fixed in paraformaldehyde were used for immunohistochemical experiments. Briefly, these sections were deparaffinized, hydrated, and incubated with a specific mouse monoclonal anti-PCNA (*proliferating cell nuclear antigen*) antibody (Santa Cruz Biotechnology), diluted 1:200 in PBS overnight at 4 °C. After washing in PBS, sections were incubated with a biotinylated secondary anti-mouse antibody (Millipore) for 2 h at room temperature, followed by Extra Avidin Peroxidase (Sigma–Aldrich) for 90 min. Staining was revealed by incubating in 0.04% 3,3′-diaminobenzidine in the presence of nickel ammonium sulfate to intensify the staining. The number of positive cells was determined by selecting

at least five areas of 300 μm^2 of uterine epithelial cells, from three sections of each animal.

Analyses of histological and histochemical images were performed on a Leica DM4000 microscope using QWinV3 program.

2.8. Statistical analysis

Data are expressed as mean ± SEM. Statistical analysis was performed by one-way ANOVA test followed by Tukey's *post hoc* test or by non-parametric Kruskal–Wallis test followed by Games-Howell's *post hoc*. Student–Newman–Keuls *t*-test was also used to determine differences between treatment means and positive or negative controls in assessments. Dose–response curves were fitted to logistic equation using nonlinear regression analysis.

3. Results

3.1. Specific fluorescent labeling with FLTX1

The cellular localization of FLTX1 labeling in MCF7 cells was analyzed by confocal laser scanning microscopy. Imaging studies on detergent-permeabilized MCF7 cells exposed to 50 μM FLTX1 showed fluorescent labeling in the cytosol, perinuclear space, and nucleus (Fig. 2A, E and G). Under non-permeabilizing conditions, fixed cells exposed to the same concentration of FLTX1 revealed a substantial fluorescence staining at the plasma membrane (Fig. 2C).

The specificity of FLTX1 binding was studied in permeabilized and non-permeabilized cells preincubated with different concentrations of Tx. These competition studies revealed that the fluorescent FLTX1 staining exhibited a dose-dependent competition with Tx, observing a partial competition at 50 μM Tx, and almost a total competition at 100 μM Tx up to 87.76 ± 3.74% in permeabilized cells (Fig. 2B and I left graph). In non-permeabilized cells, 100 μM Tx completely antagonized FLTX1 labeling at the plasma membrane (Fig. 2D and I middle graph), indicating the presence of specific binding sites for triphenylethylene compounds at the cell surface. The fluorophore (NBD-Cl) was unable to compete the FLTX1 signal (Fig. 2F), indicating that the fluorophore moiety of FLTX1 was not responsible for the fluorescent binding.

We next performed competition experiments with E2 to assess whether FLTX1 was capable to bind estradiol binding sites, including ER. In these experiments, detergent-permeabilized MCF7 cells were preincubated with increasing concentrations of E2 before the exposition to the fluorescent tamoxifen (Fig. 2H). Results showed that fluorescent signals at 50 μM FLTX1 were only partially competed with 50 μM and 100 μM E2 (up to 25.84 ± 6.36%) (Fig. 2I right panel). This inability of E2 to totally displace FLTX1 in MCF7 cells reinforces the notion that triphenylethylene compounds have the ability to interact with targets other than ER, some of which might underlie some of their undesirable side effects [13,21,22]. To further explore the relationship between FLTX1 binding and ER, we performed colocalization assays in MCF7 cells. Under permeabilizing conditions, a substantial fraction of MC-20 antibody labeled ERα colocalizes with the FLTX1 fluorescent signal (71.75 ± 2.24%), mostly at the perinuclear space (Fig. 3C and F). Interestingly, the percentage of co-localization of FLTX1 signal with the MC-20 complex was 40.12 ± 3.11%, in agreement with the notion that FLTX1 interacts with targets other than ERα. To our knowledge, these results provide the first visual evidence for the existence of non-canonical cellular targets (other than ER) for Tx, as revealed by a number of functional and pharmacological studies [21–26].

3.2. Competition studies of FLTX1 and radiolabeled estradiol on ER

Competition experiments were performed using rat uterus cytosol. This extract rich in ER was saturated with 5 nM of labeled E2 in the presence of increasing concentrations of unlabeled Tx or FLTX1 (Fig. 4A). As expected, in a dose-dependent manner, Tx was able to competitively displace the [^{3}H] E_2 from rat uterine ER. Similarly, FLTX1 competed off the radiolabeled estradiol binding to ER. The estimated IC_{50} values for Tx and FLTX1 were 123.4 ± 30.9 nM and 87.5 ± 17.5 nM, respectively. Thus, assuming a RBA (relative binding affinity) value of 100 for Tx, the value for FLTX1 was to 141.01, indicating a slightly increased affinity for ER than Tx.

3.3. Effects on MCF7 cell proliferation

Next, we compared the effects of Tx and FLTX1 on MCF7 cell proliferation (Fig. 4B). Tx and FLTX1 were exposed at concentrations ranging from 100 nM to 10 μM. In contrast to Tx (that failed to modify cell proliferation except at doses above 1 μM), FLTX1 reduced cell proliferation in a dose-dependent manner, being significantly more effective than Tx already at 0.1 μM. Tx provoked an abrupt reduction of cell growth above 3 μM and displayed a clear cytotoxic effect at 10 μM, with 23% of viable cells, as compared with 59.5% value of FLTX1 at same concentration respect to vehicle (Fig. 4B).

In order to evaluate the capacity of these triphenylethylene compounds to antagonize estradiol-induced cell proliferation, MCF7 cells were pretreated with different concentrations of Tx or FLTX1 24 h prior to the addition of 100 pM E2 for further 4 days (Fig. 4C). The results show that, like Tx, 3 μM FLTX1 was able to counteract the increase in cell growth induced by E2 down to the vehicle level. The antiproliferative effect of 10 μM FLTX1 also resulted similar to vehicle value, pointing to an inhibition of ER-mediated cell growth. However, cells pretreated with 10 μM Tx displayed a significant reduction in cell viability (26% compared to vehicle), suggesting additional cytotoxic effect triggered by Tx at the highest concentration.

3.4. Evaluation of transcriptional activity mediated by ER

Agonistic and antagonistic ER-mediated transcriptional activity was assayed using both transiently transfected MCF7 cells and stably transfected T47D-KBluc cell line, which contain estrogen response element coupled to luciferase reporter gene. Tx and fluorescent derivative were tested at different doses from 100 pM to 30 μM, for the assessments of estrogenic and antiestrogenic responses (Fig. 4D, E, respectively).

The agonistic approach showed that Tx significantly increased transcriptional activity in both cell lines, in a dose-dependent manner from 10 nM to 1 μM in MCF7 and from 10 nM to 3 μM in T47D-KBluc cells (Fig. 4D). Maximal estrogenic activities (around 2.5–3-fold) were found between 10 nM and 300 nM in both cell lines. Conversely, FLTX1 was devoid of ability to stimulate luciferase transcriptional activity in MCF7 cells. In T47D-KBluc cells, a slight yet significant increment (1.4- and 1.25-fold), was found between 100 pM and 1 nM. Besides, FLTX1 reduced luciferase expression below control values in a dose-dependent manner, at concentrations above 100 nM in T47D-BKluc cells and above 1 μM in MCF7 cells. This reduction was not mimicked by Tx, even at highest dose, in either cell lines (Fig. 4D). The decreasing effect in luciferase expression by FLTX1 did not involve the reduction in the amount of total protein (not shown), but rather indicates it causes a strong inhibition of ER-mediated transcriptional processes.

To assess antiestrogenic activity, tested chemicals were assayed against 100 pM E2, the lowest concentration that produced a maximal estrogenic response (data not shown). In these experiments,

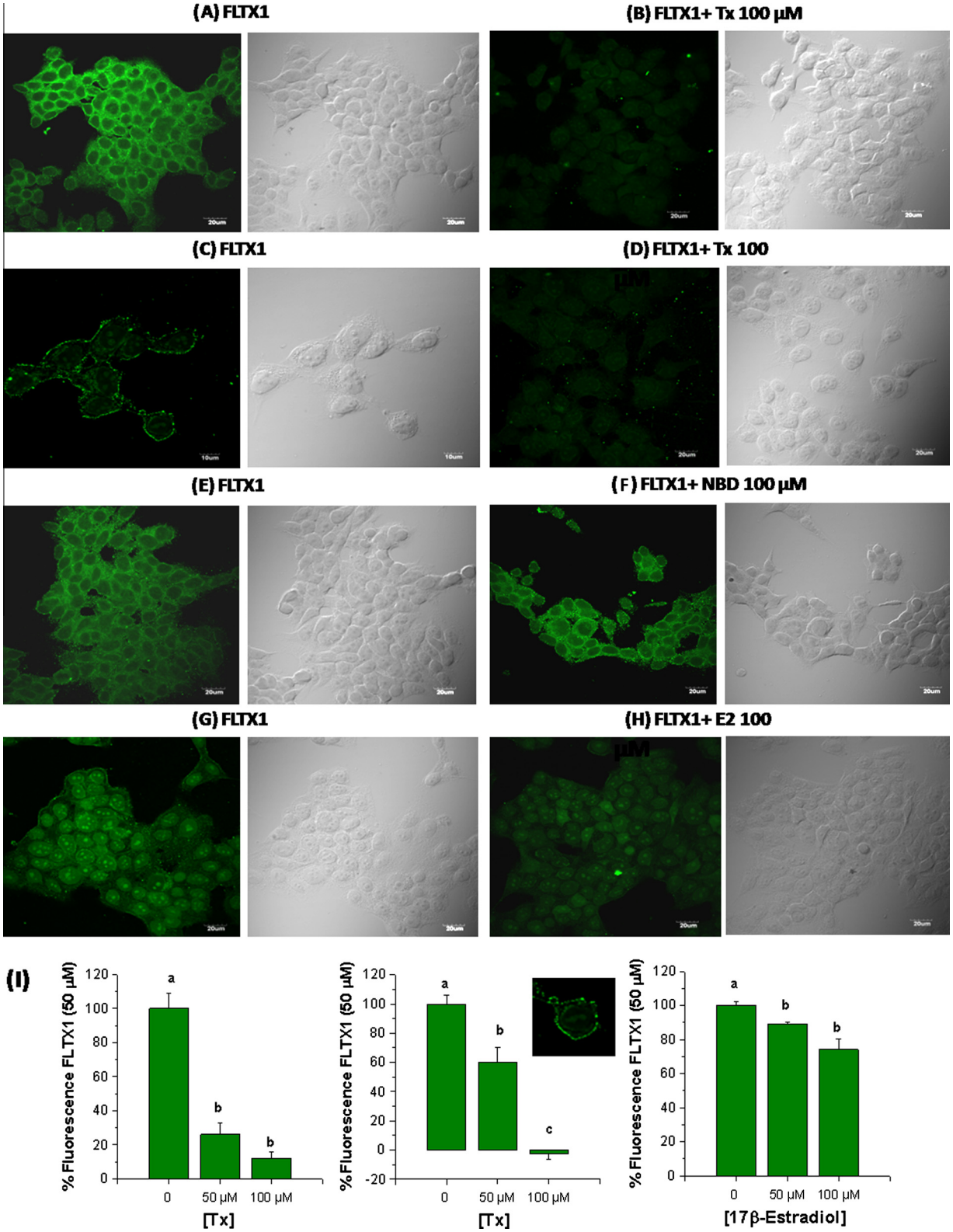

Fig. 2. Specificity of FLTX1 labeling in MCF7 cells. (A–D) Competition studies with Tx in permeabilized (A and B) and non-permeabilized MCF7 cells (C and D). The fluorophore NBD-Cl (100 µM) does not affect FLTX1 fluorescent signal (E and F). Competition of FLTX1 labeling by 17β-estradiol (G and H). Bar charts depict quantification of fluorescent pixels in cells exposed to FLTX1 and the respective treatment at the different doses used (I). Different letters indicate significant differences between doses ($p < 0.05$). (For interpretation of the references to color in this figure legend, the reader is referred to the web version of this article.)

Tx and FLTX1 decreased E2-induced luciferase activity in a dose-dependent manner in both cell lines (Fig. 4E). Estimated IC_{50} values derived from dose–response analyses were 0.73 ± 0.25 and 1.74 ± 0.95 µM for Tx and FLTX1 in MCF7 cells, respectively, and 0.33 ± 0.04 and 0.61 ± 0.03 µM for both in the case of T47D-BKluc cells.

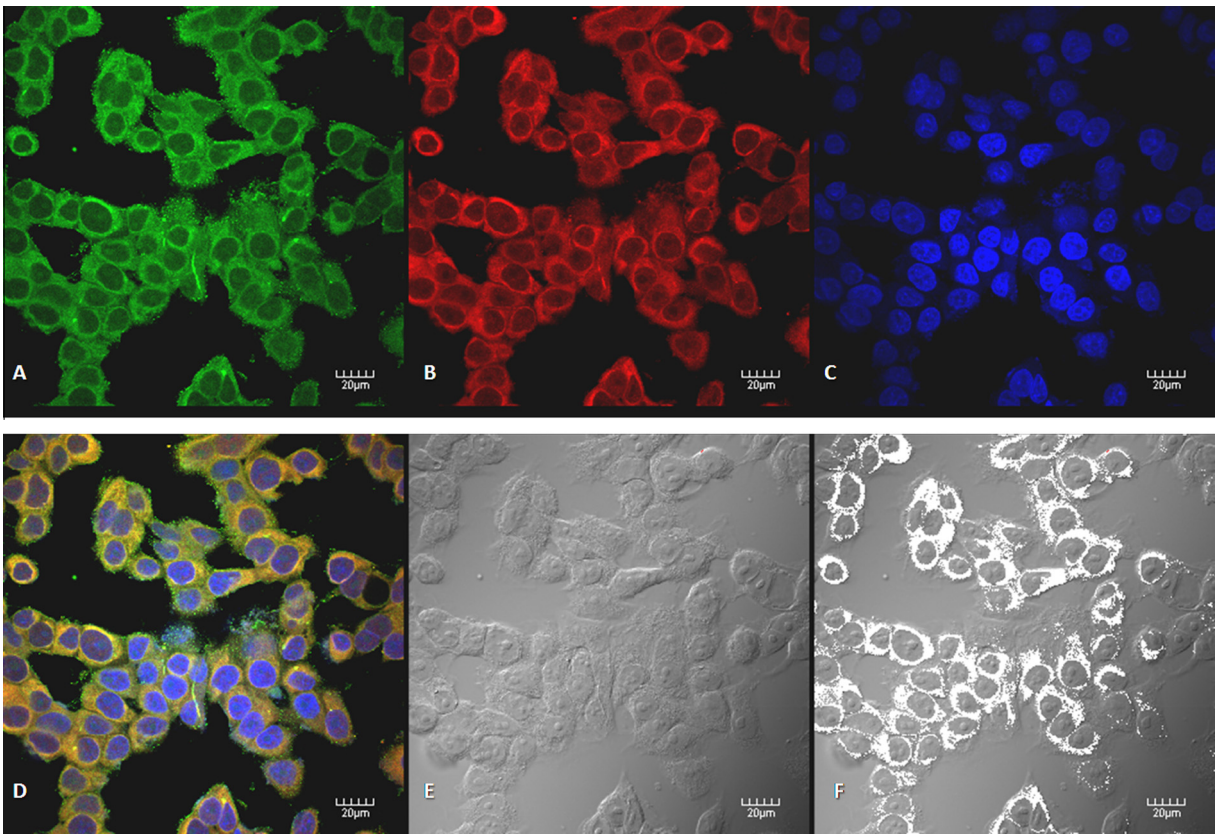

Fig. 3. FLTX1 labeling colocalizes with estrogen receptor alpha (ERα) in MCF7 cells. MCF7 cultures were incubated with FLTX1 (A) in the presence of the anti-ERα specific MC-20 antibody (B). In C, the DAPI nuclear stain. (D) Merged image of green (FLTX1), red (ERα), and blue (DAPI) staining resulting in a yellowish color is shown. Transmission image (E) overlapped with co-localization spots (F) in white.

Neither Tx nor FLTX1 displayed cross-activation of luciferase expression under the control of androgen or glucocorticoid receptors, as demonstrated in hormone responsive MDA-kb2 cell line (Supplementary material S3).

3.5. Uterotrophic assays

Immature female CD-1 mice and Sprague–Dawley rats were subcutaneously injected with oily solution containing the corresponding treatments during 3 consecutive days. Treatments did not provoke any adverse effect on the animals' health, and we did not observe any difference in body weight gain among different groups compared to vehicle.

Treatment-related effects on relative tissue weights in mice and rats are detailed in Supplementary material S4 (Tables 1 and 2, respectively). E2 and EE used as positive agonistic controls in mice and rats, respectively, induced a significant increment in uterine weights (wet, blotted, and horns), as well as cervical and vaginal weight in both animal models. No differences were found in liver and spleen weights for E2 and EE with respect to vehicle.

Results summarized in Fig. 5 show the effects of Tx and FLTX1 on uterine wet weight, cervical and vaginal weights for both mice (A) and rats (B). Uterotrophic assays in mice showed that the increases in uterine weights (wet, blotted, or horns) induced by Tx were significantly greater than with vehicle, and similar to E2 from 0.1 mg/kg, displaying the maximum uterotrophic response at this dose (Fig. 5Aa and Table 1 in Supplementary material S4), confirming the well-known agonistic effect of Tx on mice uterus [27]. Cervical and vaginal weights in Tx-treated animals were also significantly increased at 0.1 mg/kg (vaginal weight was significantly increased even at 0.01 mg/kg/day) (Fig. 5Ac and Ae). Remarkably, FLTX1 did not induce any increment in uterine (wet, blotted, or horns), cervical, and vaginal weights in the same range of doses used for Tx (Fig. 5Aa). In general, FLTX1 values remained similar or slightly lower than control vehicle values (Fig. 5A and Table 1 in Supplementary material S4).

The immature rat uterotrophic assays is an established model of partial agonist/antagonist effects for SERMs [27,28]. In the rat, 3 days treatment with Tx elicited a dose-dependent increase in uterine (wet, blotted, or horn), luminal fluid and cervical weights, which were statistically significant from 0.01 mg/kg (Fig. 5Bb and Bd and Table 2 in Supplementary material S4). Additionally, a potent estrogenic effect of Tx is observed at 10 mg/kg, where blotted uterus, horns, cervical, and vaginal weights were similar to EE-treated animals (Fig. 5Bd and Bf and Table 2 in Supplementary material S4). Unlike Tx, FLTX1 was devoid of estrogenicity until the dose of 10 mg/kg, where it significantly increased uterine wet, blotted, and horn weights, as well as luminal fluid, cervical, and vaginal weights to values equivalent 100 times less concentrated Tx (0.1 mg/kg, Fig. 5Bb), highlighting the poor potency of FLTX1 as estrogen agonist as well as the different pharmacokinetics of both compounds.

When co-administered with EE, both molecules were shown to reduce uterotrophic effect in the rat, but to different extents (Fig. 5Bb and Table 2 in Supplementary material S4). Thus, Tx values were significantly decreased from 0.01 mg/kg for wet and blotted uterine weights, or from 0.1 mg/kg in case of uterine horn weights, whereas FLTX1 only significantly reduced uterine wet weights when administered at 10 mg/kg (although a not significant 25% reduction is observed already at 1 mg/kg) (Fig. 5Bb). No significant differences were observed neither in cervical nor in vaginal weights for Tx or FLTX1 treated animals (Fig. 5Bd and Bf).

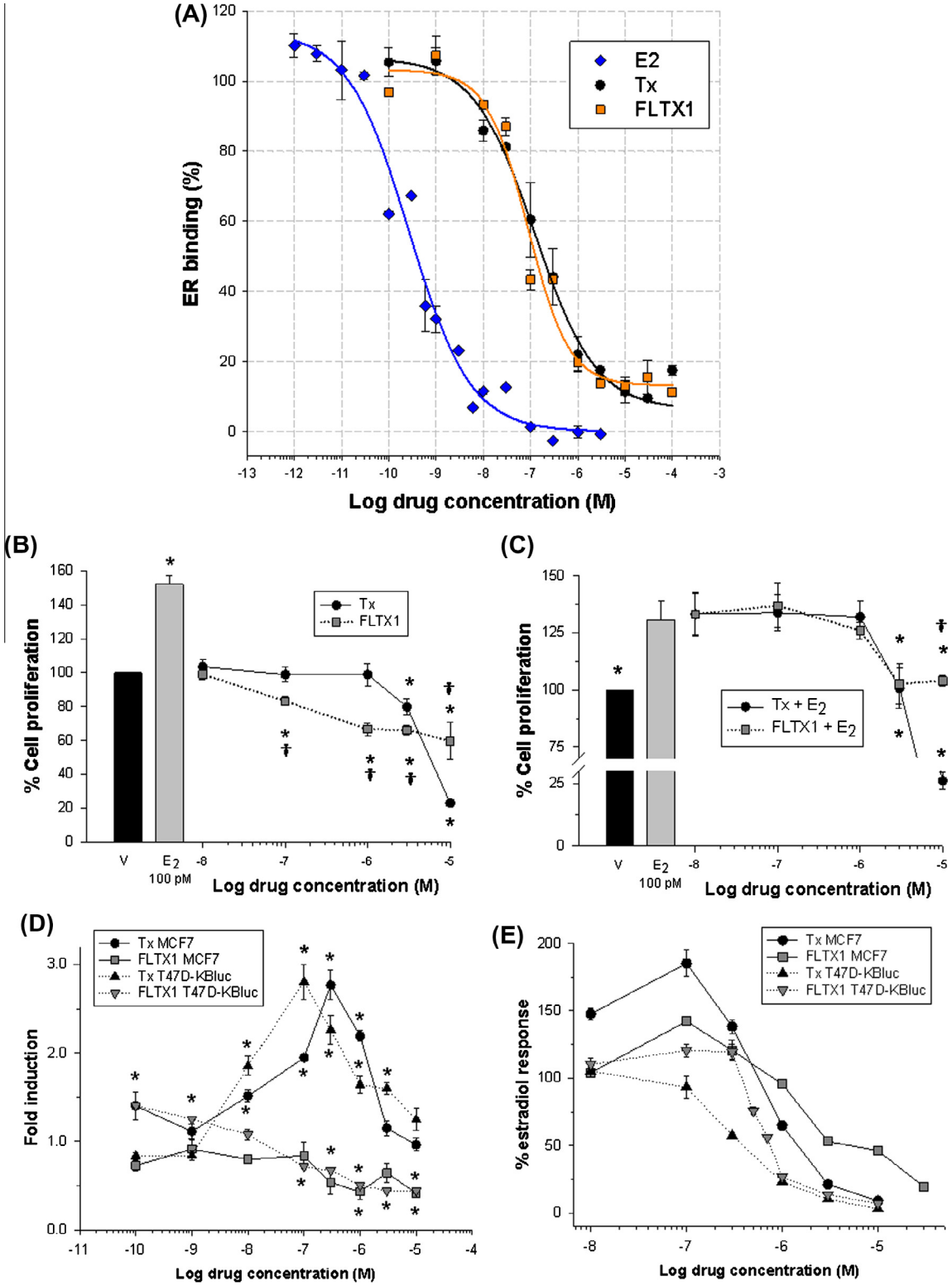

Fig. 4. (A) Effects of FLTX1 and Tx on [^{3}H]-estradiol competitive ER binding assay. Uterine cytosolic extracts were saturated with 5 nM of labeled estradiol in the presence of increasing concentrations of unlabeled competitors (0.1 nM–100 μM) for 18 h at 4 °C. Data are presented as mean ± SEM for five different assays performed for each compound and concentration. (B and C) Effects of FLTX1 and Tx on MCF7 cell proliferation assays, in the absence (B) or presence (C) of estradiol (100 pM), for estrogenic or antiestrogenic assessments, respectively. Cells were incubated for 6 days with increased concentrations (10 nM–10 μM) of triphenylethylene compounds alone (estrogenic approach) or pretreated with pretreated with FLTX1 or Tx for 24 h before addition of 100 pM 17β-estradiol (E2) (antiestrogenic approach). Values are expressed as mean percentage ± SEM over vehicle (V). $^*p < 0.05$ *vs.* control (B) or E2 (C). $^\dagger p < 0.05$ significantly different to Tx value at same dose. At least five replicate assays were used in all experiments. (D and E) Transcriptional activities of FLTX1 and Tx on transiently transfected MCF7 cells and stably transfected T47D-KBluc cell line, with estrogen response element coupled to luciferase reporter gene. Dose–response curves for agonist (D) and antagonist (E) ER-mediated transcriptional activities were determined. Data are presented as mean ± SEM fold induction compared to vehicle (D) or percent of 0.1 nM 17β-estradiol (E) response of three assays for agonist or antagonist assays, respectively. $^*p < 0.05$ compared to vehicle. (For interpretation of the references to color in this figure legend, the reader is referred to the web version of this article.)

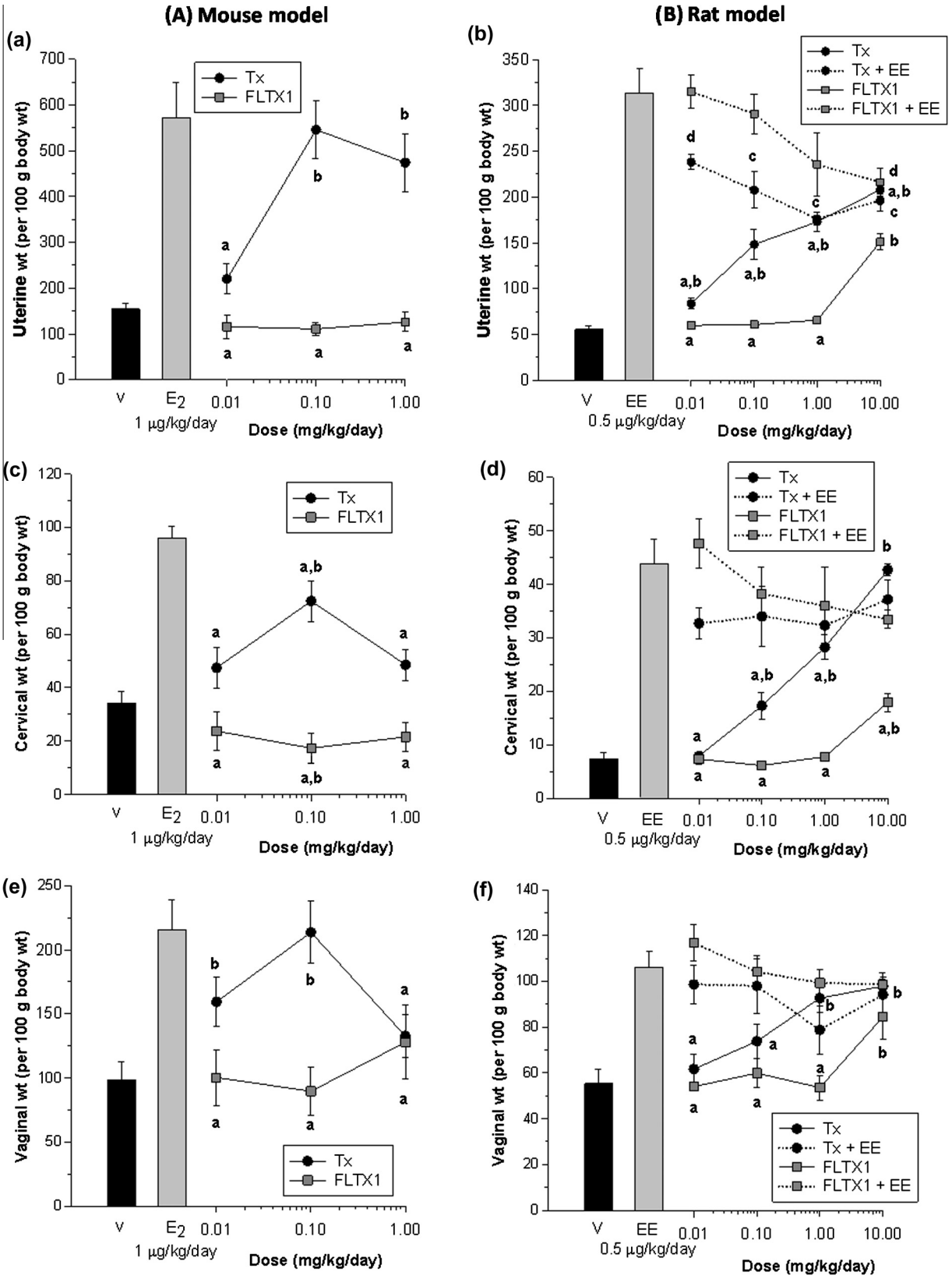

Fig. 5. Uterotrophic assays performed in immature female CD-1 mice (A) and Sprague–Dawley rats (B). Illustrated correspond to uterine wet (a and b), cervical (c and d) and vaginal (e and f) weights (per 100 g body weight) for animals injected for 3 consecutive days with indicated dosage of FLTX1 or Tx. In the rat model, the same doses of triphenylethylene compounds were also co-administrated with 0.5 µg/kg ethinyl estradiol (EE) for 3 days. Each data point represents the mean ± SEM from a minimum of five (mice) or four (rats) animals. [a] $p < 0.05$ significantly different from 17β-estradiol (E2) or EE for agonistic values in mice or rats respectively. [b] $p < 0.05$ significantly different from vehicle (V) for agonistic values. [c] $p < 0.01$; [d] $p < 0.05$ significantly different from EE for antagonistic values.

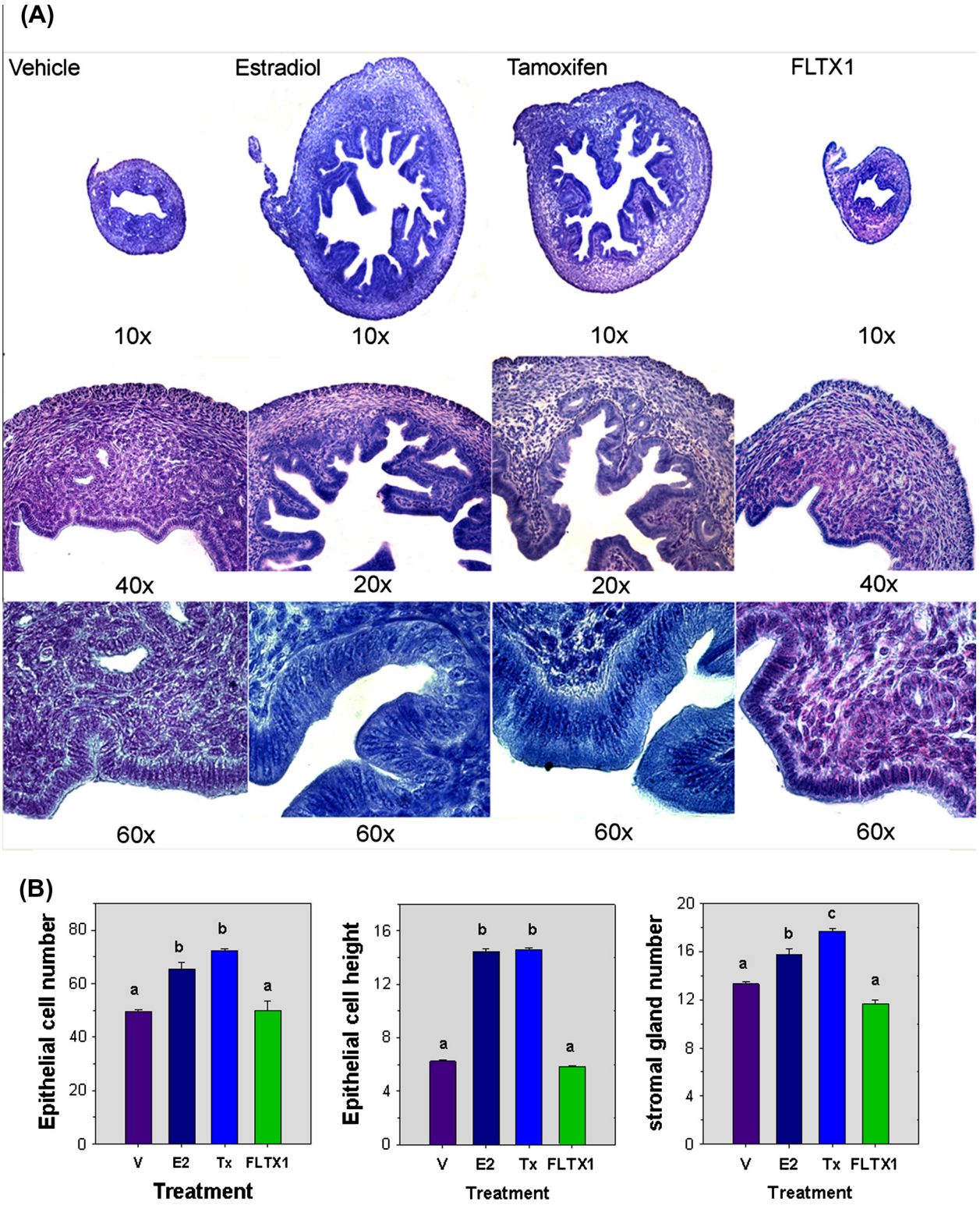

Fig. 6. Histological effects of Estradiol, tamoxifen and FLTX1 on immature mice uteri. (A) Representative Hematoxylin-eosin staining microphotographs of cross-sectional images (upper panels) in animals injected for 3 consecutive days with 1 μg/kg 17β-estradiol or 1 mg/kg/day (FLTX1 and Tx) using olive oil as vehicle. Medium panels: detailed morphological effects of hormonal treatments on uterine histology showing the myometrium (myo), stroma (stro) and epithelium (epi). Lower panels: Epithelial changes in the different experimental conditions. Magnification values are indicated. (B) Quantitative effects of E2, Tx and FLTX1 on morphological endpoints: epithelial cell number (left), epithelial height (center) and stromal gland number (right). Results are expressed as mean ± SEM from four different animals under each treatment. For methodological details see methods. Different letters indicate significant differences between treatments with $p < 0.01$. (For interpretation of the references to color in this figure legend, the reader is referred to the web version of this article.)

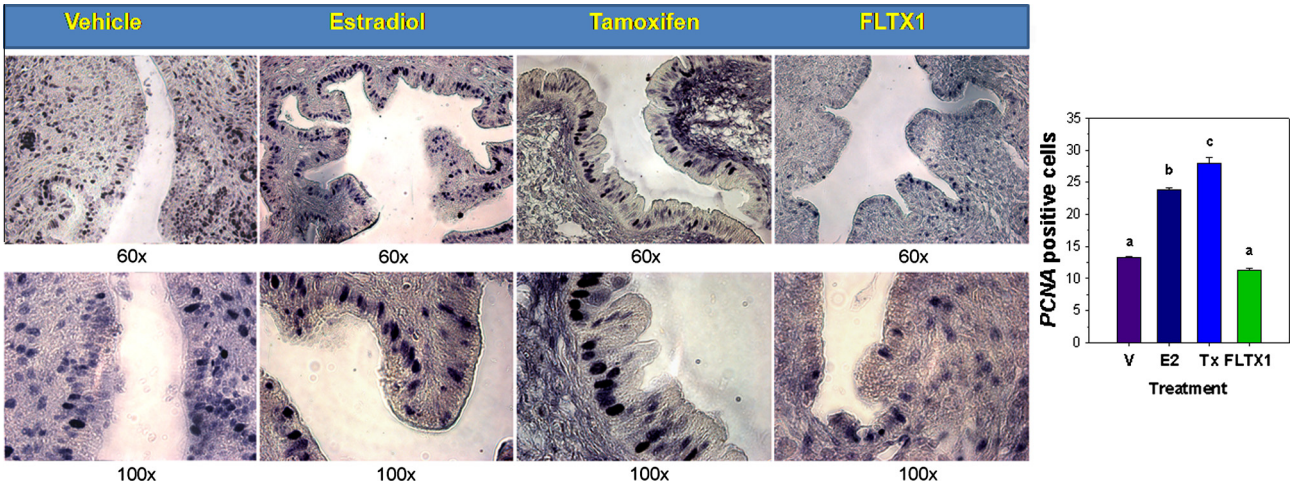

Fig. 7. Uterine cell labeling for *Proliferating cell nuclear antigen* (PCNA) in vehicle, estradiol, tamoxifen, and FLTX1 treated mice. Animals were treated as in Fig. 6. Epithelial as well as stromal labeling can be seen by the brown staining reaction. Lower panel: higher magnification of uterine epithelial layer showing the nuclear staining. Magnification values are indicated. Right panel: Quantitative effects of E2, Tx, and FLTX1 on epithelial cell immunostaining with anti-PCNA antibody. Results are expressed as mean ± SEM from four different animals under each treatment. For methodological details, see methods. Different letters indicate significant differences between treatments with $p < 0.01$.

3.6. Effects of E2, Tx, and FLTX1 on mouse uterine histology and immunohistochemistry

The uterine effects of E2, Tx, and FLTX1 on histomorphology of mouse uterus were analyzed in animals receiving olive oil (vehicle), 1 μg/kg/day E2 or 1 mg/kg/day (Tx and FLTX1), for three consecutive days. Doses were chosen according to the results from uterotrophic assays in the previous section. Fig. 6A illustrates representative hematoxylin-eosin stained uterine sections in the four experimental conditions. As can be seen, both E2 and Tx bring about a considerable increase in cross-sectional uterine size (affecting both stroma and myometrium). Conversely, FLTX1 treatment did not modify uterine size compared to vehicle. We determined three established morphometric parameters, i.e. epithelial cell height, epithelial cell number, and gland number (Fig. 6B). The results consistently demonstrated that both E2 and Tx treatments provoked a considerable increase in epithelial cell number (32.1% and 45.9% for E2 and Tx), epithelial cell height (131.5% and 134.2% for E2 and Tx, respectively), and gland number (13.3% and 18.5% for E2 and Tx, respectively), as indicatives of the uterine hypertrophic and hyperplasic effects of these molecules (Fig. 6B). In contrast to Tx, treatment with FLTX1 did not caused any significant response as compared to vehicle-treated animals, reinforcing the observation that FLTX1 is devoid of estrogenic effect in the mouse uterus.

Finally, the proliferative effects of tested compounds on uterine tissue were assessed by immunohistochemical analyses of *proliferating cell nuclear antigen* (PCNA) labeling. Results shown in Fig. 7 demonstrate that both E2 and Tx dramatically increased nuclear PCNA staining in epithelial cells (80.0% and 111.3% for E2 and Tx, respectively). Again, Tx displayed the greatest positive response among all treatments. Unlike Tx, FLTX1 failed to modify the number of PCNA-positive epithelial cells as compared to control animals (Fig. 7, right panel), which agrees with the lack of uterotrophic effects and morphometric changes of FLTX1.

4. Discussion

Fluorescent technical approaches based on modified fluorophore ligands are important tools widely used to track localization and dynamics of cellular targets in response to different drugs. This information is crucial in the case of drugs that, like Tx, display a number of important adverse effects, some unrelated to its canonical target, the estrogen receptor. That was our original goal in developing the first fluorescent tamoxifen derivative suitable for identification of non-canonical binding sites that could trigger different mechanisms and activities in non target cells [12,13,21,23,24].

To our knowledge, there is only one reported work on the development of fluorescent tamoxifen derivatives, in which a six-carbon linker was used to attach the fluorophores BODIPY, carboxyfluorescein, or Alexa Fluor 546 to 4-OH-tamoxifen [29], but the resulting fluorescent molecules displayed weaker interactions with ER than the parent molecule [29]. This suggests that excessive bulky side chains hinder the binding to the ER ligand binding pocket [29]. It is widely accepted that the triphenylethylene core of Tx is the structural motif required for interaction with the ligand binding domain of ER, while the lateral side chain is largely responsible for the antiestrogenic effects by hampering conformational activation of ER [12,17,18]. In contrast to the binding requirements for the aryl rings, the ethyl side chain of Tx protrudes out of the ER binding pocket and thus appears to be a suitable position for functionalization. In the strategy reported here, NBD dye was selected by its small size, polarity, and reactivity. This dye was directly attached onto the basic nitrogen in the alkylaminoethoxy side chain of demethyltamoxifen, while the triphenylethylene core remained intact (Fig. 1).

Labeling of FLTX1 fluorescence in unstimulated MCF7 cells was localized mainly in the cytosol, especially around the nucleus, as well as at the plasma membrane and intranuclear compartments. Further, FLTX1 labeling was totally displaced by unlabeled Tx, but only partially by 17β-estradiol, suggesting that binding sites other than ER exist for Tx in these cells. In agreement with this notion, overlapping of FLTX1 fluorescent signal and ERα immunostaining revealed only a partial colocalization for FLTX1 on ERα. The colocalization of these two molecules occurred mainly at the perinuclear level, but was also seen at the plasma membrane, in agreement with previous observations demonstrating the presence of membrane-associated ERs in different cell types, including MCF7 cells [30,31]. The main staining by MC-20 in the cytosolic and perinuclear regions of permeabilized cells was initially unexpected. However, a survey of the recent literature on the subcellular distribution of ER has revealed that our results are, indeed, in

good agreement with the balance existing for subcellular distribution of ER in MCF7 cells, and that breast cancer cell lines, especially MCF7 cells, are heterogeneous populations of cells. Thus, a recent reassessment of ER expression in human breast cancer cell lines using a variety of detection methods has demonstrated that the main location for ER (both α and β) is the cytosolic, but not the nuclear, compartment [32]. Interestingly, this comparative study also reported the common presence of ER-like immunoreactivity at the plasma membrane. A widely accepted interpretation for these findings is that ER is not permanently located in a single subcellular compartment, but it may exist in a dynamic equilibrium between the plasma membrane, cytoplasm, and nucleus [33,34].

We also found that FLTX1 was pharmacologically and biologically active. Thus, relative binding affinity for ER and IC_{50} values for FLTX1 were found to be slightly better than for Tx (actually, IC_{50} was about 30% lower and RBA 40% higher than for Tx). These properties were remarkable since, in general, changes in the side chain of Tx have led to compounds with decreased affinity for ER [29,35,36]. Furthermore, not only FLTX1 efficiently bound ER but also modulated ER-mediated transcriptional activity. Assays performed in transfected MCF7 and T47D-KBluc with luciferase reporter gene showed that both Tx and FLTX1 antagonized the estradiol-induced transcriptional activity in a dose-dependent manner and to a similar extent therefore demonstrating the ability of FLTX1 to antagonize ER-mediated transcription. However, more important, FLTX1 was devoid of the potent estrogenic agonist activity of Tx in the estrogenic assessments in both cell lines. This finding was remarkable since this estrogen-like action of Tx, perverted to an agonist, potentially mimics what happens in certain tamoxifen-resistant breast cancer [37,38]. This suggests that the attachment of the heteroatom-rich NBD group to tamoxifen aminoethoxy side chain brings about a molecule endowed with pure antiestrogen properties. This hypothesis was further explored in the estrogenic uterotrophic assays discussed below.

As expected, Tx and FLTX1 were capable to inhibit MCF7 cell proliferation. However, compared to Tx, FLTX1 displayed a higher ability to reduce cell growth rate in MCF7. E2 was capable of counteracting this antiproliferative effect of FLTX1, suggesting a direct antagonism of the fluorescent derivative on ER-mediated growth, which agrees with the results from transcriptional activation. One important difference between Tx and FLTX1 is observed at the highest concentration, where Tx, but not FLTX1, induced a dramatic decrease in cell viability well below control cells (Fig. 4C), which agrees with previous reports demonstrating tamoxifen-induced apoptosis [39,40].

The major concern in the use of Tx as adjuvant therapy in the treatment of breast cancer is the increased risk of developing uterine cancer [9,10,41,42]. Moreover, it is known that uterine growth and development is absolutely dependent on ER signaling [43–46]. Given the relevant absence of estrogenicity of FLTX1 on ER-dependent transcriptional activity, we found worthwhile to extend our studies on the regulation of uterine growth *in vivo* by the new fluorescent derivative. The rodent model of uterotrophic bioassays is particularly appropriate for the assessment of triphenylethylene derivatives, since Tx has been reported for quite long time to behave as full estrogen agonist in mouse uterus and as partial estrogen agonist/antagonist in rats uterus [4,27,28]. The reasons for this differential response to tamoxifen between both murine models are only partially understood. Recent compiled information by Smith and O'Malley [47] indicates that it is the biochemical microenvironment surrounding the estrogen receptors, i.e. the type of corregulators and their expression levels, rather than the subtype of ER, what determines the full (mouse)/partial agonist (rat) behavior of tamoxifen in the rodent uterus [47].

Remarkably, in the mice uterine model, we observed that FLTX1 lacked the uterotrophic (and also cervical and vaginal) agonistic effects of Tx [27,28]. On the other hand, in the rat model, FLTX1 only showed some sort of estrogenicity in the rat uterus, but this was only detectable at the largest dose. Overall, the results indicate that, unlike Tx, the florescent derivative is devoid of uterine estrogenicity, suggesting a differential recruitment of corregulators between Tx and FLTX1 upon binding to ER [27,28,47]. Further, on view of these results, it turns out that important differences exist between *in vitro* and *in vivo* responses to Tx and FLTX1. These differences are most likely due to the differential pharmacokinetics of both compounds.

A deeper approach on the effects of Tx and FLTX1 was achieved by histological study of uterine tissue in the same mice subjected to uterotrophic assays. This approach allowed us to assess different cellular endpoints that could be associated with endometrial carcinogenesis, i.e. epithelial cell height, epithelial cell number, stromal and myometrial sizes, gland number, and epithelial PCNA immunoreactivity, in response to estrogen/antiestrogen treatments [48,49]. Our data showed that Tx was as potent as estradiol in inducing uterine wall hypertrophy, with increased gland number, stromal and myometrial sizes, and endometrial hyperplasia, with augmented epithelial cell number and height, as previously reported [28,49,50]. Remarkably, FLTX1 completely lacked of any significant hypertrophic/hyperplasic effect, showing values comparable to vehicle-treated controls. Further, quantification of PCNA-positive epithelial cells, as indicative of active cell proliferation, revealed a potent stimulatory effect of Tx and E2, but a null effect of FLTX1, thereby emphasizing the non-mitogenic character of this novel derivative.

From the data reported in this study, it is the absence of estrogen-like effects of FLTX1 the most outstanding property of this new pharmacophore. The molecular mechanisms for this exquisite selectivity remains speculative and beyond the scope of this study. It could be hypothesized, however, that its antiestrogenic ability is mechanistically similar to that of Tx, by binding the LBD domain through its triphenylethylene core and the lateral side chain protruding out the LDB pocket and displacing helix 12 from adopting its agonist conformation [18,51]. The compact volume of NDB and its spatial conformation respect to the triphenylethylene core as indicated by the minimal-energy conformations (Fig. 1B) strongly support this notion. It could be speculated that FLTX1 may not only blocks the ER activation by estrogens but also it could downregulate the ER expression, as it has been described for other antiestrogens acting as selective estrogen receptor down-regulators (SERDs) [16]. Nevertheless, the observations that FLTX1 directly binds ER and prevents ERE-mediated luciferase expression strongly support its action on ER as the mechanism supporting the antiproliferative effect observed *in vitro* and *in vivo*. A more complex situation regards the lack of estrogenicity observed for FLTX1 in breast cancer cell lines and, in particular, in the rodent uterus. It is known that for agonist ER ligands, helix 12 is stabilized in a conformation that allows it to form one side of the coactivator-binding site [11,51]. We hypothesize that the spatial conformation of FLTX1 accommodates NBD moiety in the grove between helixes 3 and 11 so that helix 12 movement adopts a geometry resembling that of pure antiestrogen ICI182780 [52]. In this geometry, FLTX1-bound ER structure hampers the sequential recruitment of tissue-specific coregulators, including SRC-1, which is required in endometrial cells in high amounts for estrogenic agonism [53]. Computer modeling of FLTX1-ER complexes is currently in process to assess these hypotheses.

In summary, apart from its fluorescent properties that makes FLTX1 a suitable probe for studies on the molecular pharmacology of Tx, the newly developed derivative is a compound biologically and pharmacologically active. FLTX1 retains the antiestrogenic potency of Tx in breast cancer cell lines, but is largely devoid of estrogenic effects both in breast cancer cells and, more important, in

uterine tissue. These properties make this derivative a potential heir of Tx, as a pharmacophore for the chemotherapy of estrogen-dependent breast cancer.

Finally, it is worth mentioning that, in addition to its biological and pharmacological properties, FLTX1 also displays an unusual optical property as it behaves as a laser dye. Laser emission from FLTX1 is an emerging property of the new molecule since neither Tx nor NBD exhibits optical gain alone. We recently demonstrated efficient output laser-like ASE (amplified spontaneous emission) in solutions of FLTX1 in acetone and in vegetal oil, under nanosecond pulsed excitation, being the external efficiency of the ASE pulses even higher than for commercial dyes, such as Rh6G [54,55]. The potential of this new property of FLTX1 is considerable, since it paves the way to design strategies that may combine optofluidic and antiestrogenic properties of FLTX1 to improve antitumor therapeutic efficiency. We are currently investigating this potential implementation in our laboratories.

Financial support

This study was supported by Grants SAF2007-66148-C02-02 (MD), SAF2010-22114-C02-01/02 (MD/RM), SAF2009-13296-C02-02 (LFP), and CTQ2009-07109 (AB) from Spanish Ministry of Science and Innovation and European Regional Development Fund Programme. We are grateful to Fundación del Instituto Canario de Investigacion del Cancer (FICIC, Spain) for financial support in the period 2007–2012. J.M.A. was hired from FICIC.

Appendix A. Supplementary material

Supplementary data associated with this article can be found, in the online version, at http://dx.doi.org/10.1016/j.ejpb.2013.04.024.

References

[1] C.K. Osborne, H. Zhao, S.A. Fuqua, Selective estrogen receptor modulators: structure, function, and clinical use, J. Clin. Oncol. 18 (2000) 3172–3186.
[2] Z. Desta, B.A. Ward, N.V. Soukhova, D.A. Flockhart, Comprehensive evaluation of tamoxifen sequential biotransformation by the human cytochrome P450 system in vitro: prominent roles for CYP3A and CYP2D6″, J. Pharmacol. Exp. Ther. 310 (2004) 1062–1075.
[3] A.E. Wakeling, J. Bowler, Novel antioestrogens without partial agonist activity, J. Steroid Biochem. 31 (1988) 645–653.
[4] S.K. Chander, R. McCague, Y. Luqmani, C. Newton, M. Dowsett, M. Jarman, R.C. Coombes, Pyrrolidino-4-iodotamoxifen and 4-iodotamoxifen, new analogues of the antiestrogen tamoxifen for the treatment of breast cancer, Cancer Res. 51 (1991) 5851–5858.
[5] A.E. Wakeling, M. Dukes, J. Bowler, A potent specific pure antiestrogen with clinical potential, Cancer Res. 51 (1991) 3867–3873.
[6] J.X. Zhang, D.C. Labaree, G. Mor, R.B. Hochberg, Estrogen to antiestrogen with a single methylene group resulting in an unusual steroidal selective estrogen receptor modulator, J. Clin. Endocrinol. Metab. 89 (2004) 3527–3535.
[7] C.R. Overk, K.W. Peng, R.T. Asghodom, I. Kastrati, D.D. Lantvit, Z. Qin, J. Frasor, J.L. Bolton, G.R. Thatcher, Structure–activity relationships for a family of benzothiophene selective estrogen receptor modulators including raloxifene and arzoxifene, Chem. Med. Chem. 2 (2007) 1520–1526.
[8] V.C. Jordan, I. Obiorah, P. Fan, H.R. Kim, E. Ariazi, H. Cunliffe, H. Brauch, The St. Gallen Prize Lecture 2011: evolution of long-term adjuvant anti-hormone therapy: consequences and opportunities, Breast 20 (Suppl. 3) (2011) S1–S11.
[9] I. Obiorah, V.C. Jordan, Progress in endocrine approaches to the treatment and prevention of breast cancer, Maturitas 70 (2011) 315–321.
[10] V.G. Vogel, J.P. Costantino, D.L. Wickerham, W.M. Cronin, R.S. Cecchini, J.N. Atkins, T.B. Bevers, L. Fehrenbacher, E.R. Pajon, J.L. Wade 3rd, A. Robidoux, R.G. Margolese, J. James, C.D. Runowicz, P.A. Ganz, S.E. Reis, W. McCaskill-Stevens, L.G. Ford, V.C. Jordan, N. Wolmark N, National surgical adjuvant breast and bowel project update of the National Surgical Adjuvant Breast and Bowel Project Study of Tamoxifen and Raloxifene (STAR) P-2 Trial: preventing breast cancer, Cancer Prev. Res. (Phila) 3 (2010) 696–706.
[11] Y. Shang, Molecular mechanisms of oestrogen and SERMs in endometrial carcinogenesis, Nat. Rev. Cancer 6 (2006) 360–368.
[12] P. de Médina, G. Favre, M. Poirot, Multiple targeting by the antitumor drug tamoxifen: a structure–activity study, Curr. Med. Chem. Anticancer Agents 4 (2004) 491–508.
[13] M. Díaz, B. García-Marrero, J. Marrero-Alonso, R. Marín, T. Gómez, R. Alonso, Cellular and molecular basis for acute nongenomically-mediated actions of SERMs, in: A. Cano, J. Calaf i Alsina, J.L. Duenas-Diez (Eds.), Selective Estrogen Receptor Modulators: A New Brand of Multitarget Drugs, Springer-Verlag, Berlin, Heidelberg, 2006, pp. 79–102.
[14] L. Hughes-Davies, C. Caldas, G.C. Wishart, Tamoxifen: the drug that came in from the cold, Br. J. Cancer 101 (2009) 875–878.
[15] B. Seruga, I.F. Tannock, Up-front use of aromatase inhibitors as adjuvant therapy for breast cancer: the Emperor has no clothes, J. Clin. Oncol. 27 (2009) 840–842.
[16] M. Fan, E.L. Rickert, L. Chen, S.A. Aftab, K.P. Nephew, R.V. Weatherman, Characterization of molecular and structural determinants of selective estrogen receptor downregulators, Breast Cancer Res. Treat. 103 (2007) 37–44.
[17] A.M. Brzozowski, A.C. Pike, Z. Dauter, R.E. Hubbard, T. Bonn, O. Engström, L. Ohman, G.L. Greene, J.A. Gustafsson, M. Carlquist, Molecular basis of agonism and antagonism in the oestrogen receptor, Nature 389 (1997) 753–758.
[18] A.K. Shiau, D. Barstad, P.M. Loria, L. Cheng, P.J. Kushner, D.A. Agard, G.L. Greene, The structural basis of estrogen receptor/coactivator recognition and the antagonism of this interaction by tamoxifen, Cell 95 (1998) 927–937.
[19] V.S. Wilson, K. Bobseine, C.R. Lambright, L.E. Gray Jr., Development and characterization of a cell line that stably expresses an estrogen-responsive luciferase reporter for the detection of estrogen receptor agonist and antagonists, Toxicol. Sci. 81 (2004) 69–77.
[20] V.S. Wilson, K. Bobseine, C.R. Lambright, L.E. Gray Jr., A novel cell line, MDA-kb2, that stably expresses an androgen- and glucocorticoid-responsive reporter for the detection of hormone receptor agonists and antagonists, Toxicol. Sci. 66 (2002) 69–81.
[21] M. Díaz, Triphenylethylene antiestrogen-induced acute relaxation of mouse duodenal muscle. Possible involvement of Ca^{2+} channels, Eur. J. Pharmacol. 445 (2002) 257–266.
[22] J. Marrero-Alonso, B. García Marrero, T. Gómez, M. Díaz, Functional inhibition of intestinal and uterine muscles by non-permeant triphenylethylene derivatives, Eur. J. Pharmacol. 532 (2006) 115–127.
[23] X.K. Liu, A. Katchman, S.N. Ebert, R.L. Woosley, The antiestrogen tamoxifen blocks the delayed rectifier potassium current, IKr, in rabbit ventricular myocytes, J. Pharmacol. Exp. Ther. 287 (1998) 877–883.
[24] M.A. Valverde, S.P. Hardy, M. Díaz, Activation of Maxi Cl^- channels by antiestrogens and phenothiazines in NIH3T3 fibroblasts, Steroids 67 (2002) 439–445.
[25] J.L. Herrera, C. Fernandez, M. Diaz, D. Cury, R. Marin, Estradiol and tamoxifen differentially regulate a plasmalemmal voltage-dependent anion channel involved in amyloid-beta induced neurotoxicity, Steroids 76 (2011) 840–844.
[26] M. Díaz, C.M. Ramírez, J. Marrero-Alonso, R. Marín, T. Gómez, R. Alonso, Acute relaxation of mouse duodenal muscle by estrogens. Evidence for an estrogen receptor-independent modulation of excitability, Eur. J. Pharmacol. 501 (2004) 161–178.
[27] S.D. Lyman, V.C. Jordan, Metabolism of tamoxifen and its uterotrophic activity, Biochem. Pharmacol. 34 (1985) 2787–2794.
[28] P. Carthew, R.E. Edwards, B.M. Nolan, M.J. Tucker, L.L. Smith, Compartmentalized uterotrophic effects of tamoxifen, toremifene, and estradiol in the ovariectomized Wistar (Han) rat, Toxicol. Sci. 48 (1999) 197–205.
[29] E.L. Rickert, S. Oriana, C. Hartman-Frey, X. Long, T.T. Webb, K.P. Nephew, R.V. Weatherman, Synthesis and characterization of fluorescent 4-hydroxytamoxifen conjugates with unique antiestrogenic properties, Bioconj. Chem. 21 (2010) 903–910.
[30] C. Powell, A. Soto, C. Sonnenschein, Identification and characterization of membrane estrogen receptor from MCF7 estrogen-target cells, J. Steroid Biochem. Mol. Biol. 77 (2001) 97–108.
[31] R. Marin, C.M. Ramírez, M. González, R. Alonso, M. Díaz, Alternative estrogen receptors homologous to classical receptor α in murine neural tissues, Neurosci. Lett. 395 (2006) 7–11.
[32] C.H. Ford, M. Al-Bader, B. Al-Ayadhi, I. Francis, Reassessment of estrogen receptor expression in human breast cancer cell lines, Anticancer Res. 31 (2011) 521–528.
[33] A. Nadal, M. Díaz, M.A. Valverde, The estrogen trinity: membrane, cytosolic and nuclear effects, News Physiol. Sci. 16 (2001) 251–255.
[34] B. Manavathi, R. Kumar, Steering estrogen signals from the plasma membrane to the nucleus: two sides of the coin, J. Cell. Physiol. 207 (2006) 594–604.
[35] S. Wilson, P.C. Ruenitz, J.A. Ruzicka, Estrogen receptor affinity and effects on MCF7 cell growth of triarylethylene carboxylic acids related to tamoxifen, J. Clin. Endocrinol. Metab. 42 (1992) 613–616.
[36] B.S. Katzenellenbogen, I. Choi, R. Delage-Mourroux, T.R. Ediger, P.G. Martini, M. Montano, J. Sun, K. Weis, J.A. Katzenellenbogen, Molecular mechanisms of estrogen action: selective ligands and receptor pharmacology, J. Steroid Biochem. Mol. Biol. 74 (2000) 279–285.
[37] S. Ali, R.C. Coombes, Endocrine-responsive breast cancer and strategies for combating resistance, Nat. Rev. Cancer 2 (2002) 101–112.
[38] J. Shou, S. Massarweh, C.K. Osborne, A.E. Wakeling, S. Ali, H. Weiss, R. Schiff, Mechanisms of tamoxifen resistance: increased estrogen receptor-HER2/neu cross-talk in ER/HER2-positive breast cancer, J. Natl. Cancer Inst. 96 (2004) 926–935.
[39] R.R. Perry, Y. Kang, B. Greaves, Effects of tamoxifen on growth and apoptosis of estrogen-dependent and -independent human breast cancer cells, Ann. Surg. Oncol. 2 (1995) 238–245.
[40] S. Mandlekar, A.N. Kong, Mechanisms of tamoxifen-induced apoptosis, Apoptosis 6 (2001) 469–477.

[41] J.I. MacGregor, V.C. Jordan, Basic guide to the mechanisms of antiestrogen action, Pharmacol. Rev. 50 (1998) 151–196.
[42] R.M. O'Regan, A. Cisneros, G.M. England, J.I. MacGregor, H.D. Muenzner, V.J. Assikis, M.M. Bilimoria, M. Piette, Y.P. Dragan, H.C. Pitot, R. Chatterton, V.C. Jordan, Effects of the antiestrogens tamoxifen, toremifene, and ICI 182,780 on endometrial cancer growth, J. Natl Cancer Inst. 90 (1998) 1552–1558.
[43] J. Gorski, D. Toft, G. Shyamala, D. Smith, A. Notides, Hormone receptors: studies on the interaction of estrogen with the uterus, Recent Prog. Horm. Res. 24 (1968) 45–80.
[44] E.V. Jensen, E.R. DeSombre, Estrogen-receptor interaction, Science 182 (1973) 126–134.
[45] J.H. Clark, B.M. Markaverich, The agonistic and antagonistic effects of short acting estrogens: a review, Pharmacol. Ther. 21 (1983) 429–453.
[46] K.S. Korach, J.F. Couse, S.W. Curtis, T.F. Washburn, J. Lindzey, K.S. Kimbro, E.M. Eddy, S. Migliaccio, S.M. Snedeker, D.B. Lubahn, D.W. Schomberg, E.P. Smith, Estrogen receptor gene disruption: molecular characterization and experimental and clinical phenotypes, Recent Prog. Horm. Res. 51 (1996) 159–188.
[47] C.L. Smith, B.W. O'Malley, Coregulator function: a key to understanding tissue specificity of selective receptor modulators, Endocr. Rev. 25 (2004) 45–71.
[48] R.R. Newbold, W.N. Jefferson, E. Padilla-Banks, V.R. Walker, D.S. Pena, Developmental Endocrinology Studies Group, Cell response endpoints enhance sensitivity of the immature mouse uterotropic assay, Reprod. Toxicol. 15 (2001) 245–252.
[49] P. Carthew, R.E. Edwards, B.M. Nolan, Uterotrophic effects of tamoxifen, toremifene, and raloxifene do not predict endometrial cell proliferation in the ovariectomized CD1 mouse, Toxicol. Appl. Pharmacol. 158 (1999) 24–32.
[50] P. Carthew, R.E. Edwards, B.M. Nolan, E.A. Martin, L.L. Smith, Tamoxifen associated uterine pathology in rodents: relevance to women, Carcinogenesis 17 (1996) 1577–1582.
[51] K.W. Nettles, J.B. Bruning, G. Gil, E.E. O'Neill, J. Nowak, Y. Guo, Y. Kim, E.R. DeSombre, R. Dilis, R.N. Hanson, A. Joachimiak, G.L. Greene, Structural plasticity in the oestrogen receptor ligand-binding domain, EMBO Rep. 8 (2007) 563–568.
[52] L.A. Paige, D.J. Christensen, H. Grøn, J.D. Norris, E.B. Gottlin, K.M. Padilla, C.Y. Chang, L.M. Ballas, P.T. Hamilton, D.P. McDonnell, D.M. Fowlkes, Estrogen receptor (ER) modulators each induce distinct conformational changes in ER alpha and ER beta, Proc. Natl. Acad. Sci. USA 96 (1999) 3999–4004.
[53] Y. Shang, M. Brown, Molecular determinants for the tissue specificity of SERMs, Science 295 (2002) 2465–2468.
[54] F. Lahoz, C. Oton, D. López, J. Marrero-Alonso, A. Boto, M. Díaz, Whispering gallery mode laser based on antitumor drug-dye complex gain medium, Opt. Lett. 37 (2012) 4756–4758.
[55] F. Lahoz, C. Oton, D. López, J. Marrero-Alonso, A. Boto, M. Díaz, High efficiency amplified spontaneous emission from a fluorescent anticancer drug–dye complex, Org. Electron. 14 (2013) 1225–1230.